THE AMERICAN SOCIETY OF MECHANICAL ENGINEERS
345 E. 47th St., New York, N.Y. 10017

98-GT-282

AN EXPERIMENTAL EXAMINATION OF CANTILEVERED AND SHROUDED STATORS IN A MULTISTAGE AXIAL COMPRESSOR

M. Swoboda[1], P. C. Ivey[2], U. Wenger[1], V. Gümmer[1]

[1] BMW Rolls-Royce GmbH
Eschenweg 11, 15827 Dahlewitz, Germany

[2] School of Mechanical Engeneering
Cranfield University
Bedfordshire, MK43 OAL, UK

ABSTRACT

This paper presents experimental investigations on a large-scale low-speed compressor facility with four repeating stages equipped with CDA-profiles (Controlled Diffusion Airfoils). Two different builds were investigated. Both builds used identical rotors, but had stators configured either in cantilevered or in shrouded form.

Traverse measurements of total pressure and flow angle at six axial locations (IGV, two rotor and three stator exit planes) were performed between 1% and 99% annulus height and across two blade pitches. Circumferentially mass-averaged radial profiles were used in a through-flow code for reconstruction analysis of the measurements. In addition to the traverse measurements surface static pressures on stage 3 rotor and stator were measured.

The effect of the „free-end" configuration on an embedded stage of this multistage compressor is described and compared to the shrouded configuration. The objective of this study was to investigate the differences of these two configurations and especially the effects caused by the hub clearance vortex in the cantilevered case.

The entire set of measurements and through-flow analysis was performed at two operating points of the compressor i.e. at peak efficiency and near stall condition. Thus also the effects of the hub clearance vortex which influences the stall margin of the compressor are described. The analysis of the results shows slightly higher pressure rise coefficients for shrouded stators, but slightly higher stall margin in the cantilevered case. This is due to a stabilizing effect of the hub clearance vortex (cleans up separation on hub) in the cantilevered configuration because its direction is opposite to the secondary flow in the passage.

NOMENCLATURE

H	total enthalpy
P	static pressure
P_t	total pressure
P_{ref}	reference pressure
U_{mid}	blade speed at mid height
V_a	axial velocity
d_{le}, d_{te}	leading edge, trailing edge diameter
d_{max}	maximum blade thickness
h	blade height
t	tip/hub clearance height
c_p	pressure coefficient: $(P_t-P_{ref})/\,{}^1/_2\rho U_{mid}^2$
ρ	density
η	efficiency
ψ	loading coefficient: $\Delta H/U_{mid}^2$
φ	flow coefficient: V_a/U_{mid}
Re	Reynolds number

INTRODUCTION

In the course of a collaborative research project on civil core compressor aerodynamics two different builds have been investigated on the four repeating stage Low Speed Research Compressor (LSRC) at Cranfield University. The intention of this project was to investigate both, rotor tip clearance flow and stator leakage effects for cantilevered (hub clearance) and shrouded configuration. This paper describes, discusses and compares the overall characteristics, area traverses and static pressure distribution of both, the cantilevered and shrouded build measured with conventional pneumatic probes

In addition to the pneumatic traverse measurements, two advanced measuring techniques were employed. Laser-2-Focus

Presented at the International Gas Turbine & Aeroengine Congress & Exhibition
Stockholm, Sweden — June 2–5, 1998

measurements were performed around and within the rotor 3 tip clearance passage region and traverses of the rotor 3 exit flow in relative frame of reference using rotating pneumatic probes. These advanced measurements on this configuration (L2F measurements and pneumatic measurements in rotating frame) are reported in a related paper by Ivey et al., 1997.

Leakage effects play a dominant role for the performance and stall margin of axial compressors. Many experimental studies have been carried out in the past on single (Goto, 1991) and multi-stage compressors (Jefferson et. al., 1958, Howard et al., 1994 and Wellborn et al., 1996 at low speed and Thomson et al., 1997 at high speed) employing different measurement and analysis techniques. The understanding of the highly viscous leakage effects is very important when using 3D Navier Stokes flow solvers in the compressor design procedure. Therefore very accurate data is needed for validation of these solvers. The currently available 3D design techniques can help to achieve higher component efficiencies (LeJambre et al., 1995) and further advances in compressor design.

Although a lot of studies deal with rotor and stator tip clearances and associated effects, there is, however, almost no work published comparing directly effects of stator hub clearances with shroud leakage flows at comparable levels of leakage i.e. the same amount of radial stator clearance and seal tooth clearance. Nikolos et al., 1995 is an example of basic research work investigating relative wall motion which is valid as well for tip and hub clearances. Adams, 1988 presents flow visualization results of cantilevered stator leakage flows. A lot of published work exists, dealing with different shroud configurations. Brankiewicz et al., 1998 investigate experimentally the impact of hub leakage flow associated with the clearance gaps of hub shrouded variable geometry stator rows and Jung et al., 1995 present investigations on stator exit flow fields for different variable stator configurations with variations in geometry of the radial clearance at the casing resulting in different structures and effects of the clearance flow. Heidegger et al., 1996 is an example of numerical work investigating the impact of different seal configurations on a shrouded stator performance.

COMPRESSOR DESIGN

The investigated blading of the low speed compressor facility LSRC with repeating stage blading was designed to be representative for the rear stages of a high pressure compressor where leakage effects play a dominant role. The stage loading was ψ=0.35 at a flow coefficient of φ=0.5. These values are valid for stage 3 which is the stage under investigation for the presented compressor. The blading design is reported by Swoboda et al.

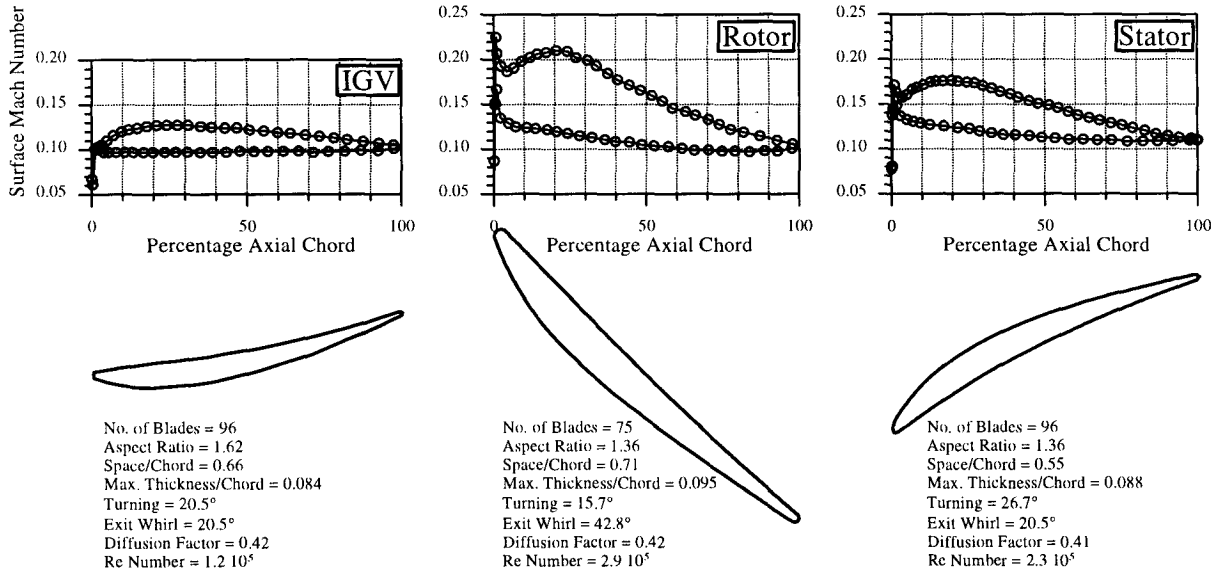

Massflow	**12.04 kg/s**	**Stage Loading**	**0.35**
Inlet Pressure	**101.28 kPa**	**Flow Coefficient**	**0.5**
Inlet Temperature	**288.15 K**	**Stage Pressure Ratio**	**1.017**
Rotational Speed	**1100 rpm**	**Degree of Reaction**	**0.64**

Figure 1: Midspan profiles of IGV rotor and stator and the respective design Mach number distribution and airfoil/stage aerodynamic loading parameters

In Figure 1 the IGV, rotor and stator blades can be seen together with some aerodynamic details and the blade Mach number distribution resulting from design blade-to-blade calculation. The low speed controlled diffusion airfoils are designed via camberline and thickness distribution to give a velocity distribution typical of high speed rear stage blades. The surface Mach number is, in the case of incompressible flow, equivalent to the velocity distribution. To ensure that the leading and trailing edges of this blading are representative to rear stages of a relatively small core compressor they are relatively thick in the present design. The relative diameter (related to max. thickness) of the leading edge in the case of the rotor d_{le}/d_{max}=0.32 (stator d_{le}/d_{max}=0.30) and the trailing edge value is here d_{te}/d_{max}=0.22 (stator d_{te}/d_{max}=0.20). The inlet guide vane (IGV) was designed to give the desired rotor inlet swirl conditions of 20.5° (measured against axial direction).

EXPERIMENTAL APPARATUS AND INSTRUMENTATION

In the course of the project a variety of experimental investigations were performed. The measurements were carried out on a four- stage low speed research compressor facility (LSRC) in Cranfield (CIT) which is described in detail by Robinson (1985, 1991). This facility offers the opportunity of very detailed measurements because of it's large physical size. The outer diameter of the compressor of 1.22m makes it possible to carry out traverse measurements in between the blade rows and very close to the annulus walls. The mechanical arrangement of the facility allows rotation of the rotor casing rings relative to the stator rings, thus enabling circumferential traversing of pneumatic probes without any disturbance of the flow near the annulus walls (no circumferential probe slot is needed). A complete set of traverse measurements over almost two stator pitches was carried out upstream and downstream of stage 1 and stage 3 rotors and stators (behind IGV, rotor 1, stator 1, stator 2, rotor 3 and stator 3). The whole measurement grid contains 29 radial and 59 circumferential points. The radial distribution is refined in the near wall region for better resolution of viscous end wall effects there. The circumferential point distribution is equally spaced over 7.3° which corresponds to 1.97 pitches of the stator. A pneumatic cobra probe was used in a manual yaw-angle mode for the whole traverse measurements, see Howard et al., 1994. The cobra probes were calibrated in a wind tunnel prior to the measurements. To achieve good accuracy two measurements were taken for every measurement point. In the first measurement the flow angles were measured roughly (according to the distinct probe calibration) by aligning the probes to the design outlet angles. In the second measurement the probes were adjusted to these measured angles for an accurate measurement of the flow angle, again according to the distinct probe calibration. The accuracy of the cobra probe in determining the swirl angle is ±0.5°. The accuracy and stability of a wedge probe would be of course much better, but in this case is not possible to carry out measurements very close to the walls because of the high radial dimension of a wedge probe. Howard et al. (1994) shows that the trends of measured flow angle and loss due to 3D effects are the same for cobra and wedge probes.

The axial traversing positions can be seen in Figure 2 together with the principal sketch of the annulus and it's dimensions.

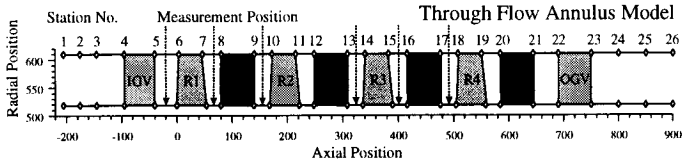

Figure 2: Principal sketch of the LSRC annulus and position of traverse measurements (Dimensions in mm)

The third stage blades, rotor and stator were instrumented with pressure tappings. Each blade accommodates 5 instrumented heights, each of those having 17 taps on the suction and 9 taps on the pressure side (5%, 10%, 50%, 94% and 97% height on rotor and 2%, 5%, 50%, 90% and 95% height on stator). Thus the regions of interest, i.e. rotor tip and stator hub can be examined in detail. All pressures are presented as a pressure coefficient representing the difference between the actual measured pressure (P or P_t) and the actual ambient reference pressure P_{ref} in front of the compressor related to the dynamic head $^1/_2\rho U_{mid}^2$ where U_{mid} is the blade speed at blade mid height. This is common practice when studying incompressible flows with small pressure changes. The uncertainty analysis for the performance and traverse data is reported by Robinson (1991) and yields to ±20Pa for deduced total pressure.

	Results Reported	**Results Reported**	**Ref.: Ivey**	**Ref.: Ivey**
	Build BRR1 Rotors t/h=2.0% Stators t/h=1.1%	**Build BRR2 Rotors t/h=2.0% Stators shrouded**	**Build BRR2 Rotating Traverse**	**Build BRR2 Laser-2Focus**
Peak Efficiency	Blade Pressures Traversing Averaging (Angle, Ptotal) Through Flow	Blade Pressures Traversing Averaging (Angle, Ptotal) Through Flow	Traversing R3 Averaging (Angle, Ptotal)	Traversing R3 Tip Clearance
Near Stall	Blade Pressures Traversing Averaging (Angle, Ptotal) Through Flow	Blade Pressures Traversing Averaging (Angle, Ptotal) Through Flow		

Table 1: Overview of all measurements carried out in the current measuring campaign

All traverse measurements were carried out at two operating points of the compressor, one at the peak efficiency and an-

other at near stall operating point. The operating points were controlled via online measurement of the overall performance, which was measured by conventional means with torque meter and calibrated inlet. Details of overall performance measurement are given by Robinson (1985). Table 1 gives an overview of the entire measurements carried out in the course of this measurement campaign.

Figure 3 shows a principal sketch of the stator in the case of the shrouded build. The shroud ring is sealed against the rotor drum by double-knife labyrinth seal. The seal tooth clearance was 1mm (1.1% blade height). In the case of the cantilevered build the shroud box is filled by another shroud ring which is rotating with the drum. The hub clearance value for the cantilevered build was chosen to be also 1.1% of blade height. Moreover figure 3 shows the axial position and the measure of the traversed cobra probe (probe head 3x1mm) which is located between the blade rows.

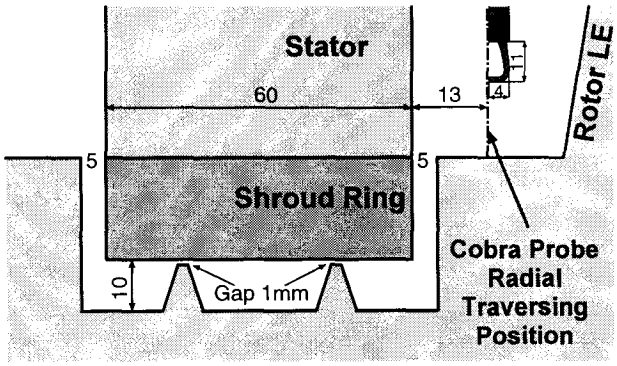

Figure 3: Principal sketch of the shroud; axial position and measure of the cobra probe (Dimensions in mm)

OVERALL PERFORMANCE

The compressor characteristics were measured by means of a torque device and calibrated inlet prior and post every traverse measurement. The throttle valve closure rate and the close increment are adjusted in such a manner that it is possible to drive the compressor with increments of the flow coefficient of $\Delta V_a/U_{mid}=0.001$ and thus the stall margin can be found very accurately. Figure 4 shows an extract of the overall compressor performance of the LSRC. Work and pressure coefficient as well as the efficiency are plotted versus the flow coefficient and compared for the cantilevered and shrouded build. Moreover, Figure 4 shows the positions of the two operating points investigated and additionally the point for which the blading was designed is indicated. It can be seen that the design point represents almost the peak efficiency point and agrees very well with the measured value of the work coefficient.

The differences between the two builds are very small in terms of pressure and work coefficient. The work coefficient is slightly higher in the shrouded case over the whole range of the flow coefficient. There are considerable differences in the efficiency levels of the two builds. The peak efficiency of the cantilevered build (over 90%) is approximately 1% higher than for the shrouded build (89%) which is surprising. The overall characteristics measurements were investigated in detail by Camp (1996). The result of this investigation showed a big scatter in efficiency measurement due to uncertainties in torque measurement accuracy. The conclusion for the peak efficiency measurement point is as follows:

Cantilevered Build BRR1: $\eta = 88.9\% \pm 0.7\%$

Shrouded Build BRR2: $\eta = 89.3\% \pm 1.2\%$

As can be clearly seen from these numbers, there is too large uncertainty to make a clear statement which is the more efficient build. The scatter which caused the uncertainty in efficiency measurement could not be investigated during this measurement campaign.

In Figure 4 the stall drop-in points can be seen for both builds. The stall point was determined by throttling the compressor to an unstable condition in the increments given above. The stall point for the cantilevered build is at a slightly lower flow coefficient, thus the stall margin is slightly higher in this case. This fact will be confirmed later when discussing the traverse measurements at near stall operating point.

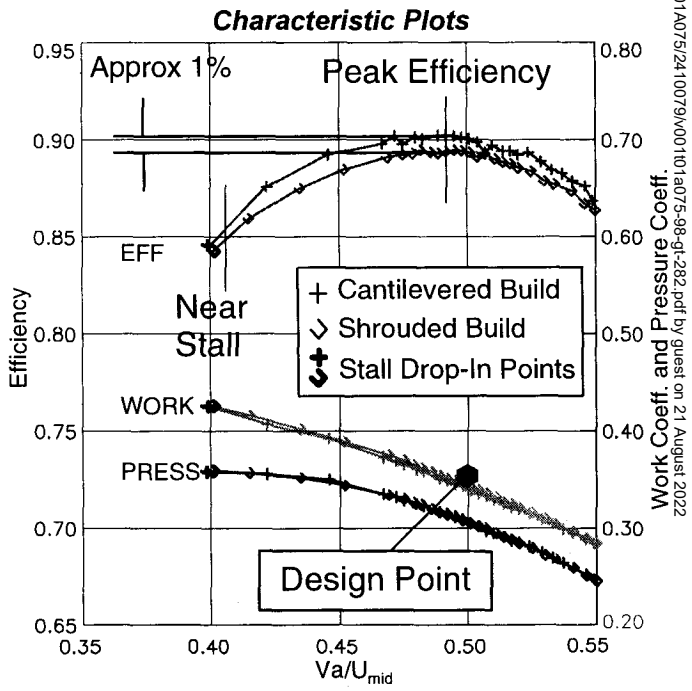

Figure 4: Overall performance of the LSRC, comparison of characteristic plots for cantilevered and shrouded build

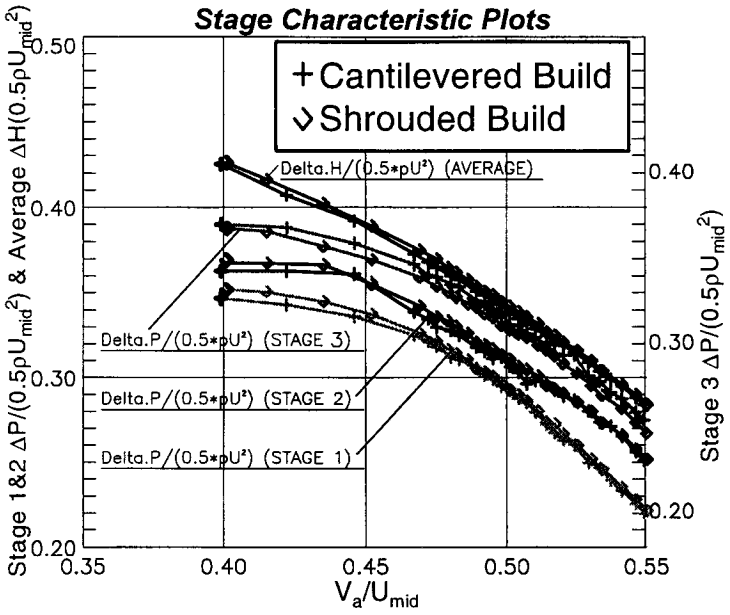

Figure 5: Overall performance of the LSRC, comparison of stage pressure rise (Stage 1, 2 and 3) for cantilevered and shrouded build

Figure 5 shows the stage characteristic plots in terms of stage pressure rise related to dynamic head versus flow coefficient, again as a comparison for both, the cantilevered and shrouded build. The pressure rise for each stage was determined at from the average of 5 circumferential positions of casing statics. For simplification only pressure rise for stage 1, 2 and 3 is shown. Note the shifted scale for stage 3 on the right hand side. The stage characteristics show an interesting behavior in the near stall region, especially in the case of stage 2. When comparing qualitatively the distributions of stage 2 to stage 1 and 3 an almost constant behavior in the static pressure rise coefficient at V_a/U_{mid}=0.43-0.44 is recognizable towards the stall point for both, the cantilevered and shrouded build. Qualitatively the distributions of stage 1 and 3 are similar. It can be stated here that stage 2 is the stage at which unstable operating conditions of the compressor occur first. This might be one of the general features of the LSRC because it is valid for both builds. This fact will be confirmed later when discussing the traverse results at near stall.

ANALYSIS TECHNIQUES

The entire traverse data (total pressure and flow angle) at all measured planes was taken through a circumferential mass momentum averaging procedure according to Dring et al., 1989. Dring recommends this procedure because the results are theoretically independent of the axial location of the traversing planes (fully mixed out flow). This procedure enables the direct determination of total pressure losses and deviation across the stators. To calculate the losses and deviation across the rotors requires the calculation of total pressure and angles in relative frame of reference. This would require the determination of the radial static pressure distribution from the calibration procedure of the cobra probe. Since the probe calibration is made in a wind tunnel, the static pressure readings in a real machine are not accurate enough to determine the relative conditions. Howard et al. (1994) report this behavior by comparing the radial static pressure profiles with static pressure on casing which do not match. For that reason the radial mass and momentum averaged profiles of total pressure and flow angles were used as a boundary condition and were fed into a through-flow model to determine all derived radial values (circumferentially averaged). The code used is a through-flow method from Denton and it is a part of the measurement and analysis system. This implies, as any through-flow method, that the circumferential variation of static pressure and all derived values must be ignored. The whole procedure is described in detail by Howard et al. (1994).

COMPARISON OF TRAVERSE DATA

Peak Efficiency Operation

Figure 6 shows the measured absolute flow angles for both, the peak efficiency and the near stall point and for both builds. On the upper side the results for peak efficiency and on the lower side those for near stall can be seen.

When comparing flow fields for the cases of cantilevered and shrouded stators there are in general two effects or differences in the structure of the flow field in the near hub region. On one hand a hub clearance vortex occurs in the cantilevered stator case which interacts with the main flow. On the other hand in the case of the shrouded stator an interaction of the main flow with the shroud ring boundary layer flow and with the shroud box leakage flow takes place. Both effects are of highly viscous character and they play a dominant role for end wall flow development.

Comparing the flow angle contours for the three stators at peak efficiency it can be seen in both cases that the end wall flow structures are migrating from the end wall into the main flow. Clearly to be seen is the increased size of a region of lower angle values in the case of the cantilevered build (near hub pressure side). This region influences the passage flow up to approximately 25-30% of blade height (from hub to tip) behind stator 3.

Comparing the tip region it becomes obvious that the flow structures are very similar in both cases. The flow field behind the shrouded stators is almost symmetrical to the mid span height, except the direct near hub region.

Considering the traverses behind the rotors in both cases distinct circumferential variations are clearly recognizable. These variations are caused on one hand by the wakes of previous stators which are migrating through the rotor row but on the other hand they can also be caused by the potential effect of the downstream stators. To isolate both effects would require to change the circumferential position of the stator rows relative to each other without moving the probe, however, it is not possible to investigate this clocking effect in this compressor and thus a quantitative split of both effects is not possible.

The thicker boundary layer on the hub of rotor 3 can be seen on the cantilevered stator case. The reason for this is the completely different structure of the hub flow in the two cases. The flow in the near hub region is continuously accelerated by the rotating hub in the case of the cantilevered stator build and the leakage below the stators is rolling up and is forming a vortex migrating from the hub to the main flow. In the case of the shrouded build the influence to the main flow is caused by the deceleration in the boundary layer when the flow is entering the steady passage of the shrouded blade and a re-acceleration caused by the rotating hub behind the shroud ring (compare figure 3). The hub boundary layer develops new and is therefore thinner in that region. This would apply to a case with perfectly sealed shroud ring. In practice there is of course also a shroud leakage flow interacting with the main flow which is very difficult to quantify.

In Figure 7 the corresponding measured total pressure traverses for all measurement planes are shown. The total pressure coefficient is of course of different level for each row, however, for comparison reasons the contours are plotted using the same pressure coefficient increment range.

When comparing the stators, a low energy region can be seen near the hub (10 to 30% blade height) growing toward the rear stages and influencing the main flow for the cantilevered build. Qualitatively similar loss region can also be found in the case of the shrouded build behind stator 1 indicating that the hub clearance vortex caused by the IGV (cantilevered in both cases) is migrating through the rotor row. This structure is smeared out behind stator 2 and 3 in the shrouded case whereas in the cantilevered case the stator hub clearance vortices seem to increase this loss region towards the rear stages.

The flow behind stators in the tip region seems not to be affected at all by the effects on the hub. The growing flow structures on the tip are similar for both builds and behind every stator. However, the overall total pressure level is slightly smaller for the cantilevered build. This applies also to the traverses behind rotor 1 and 3. In both cases again a circumferential variation can be seen as well in the main flow field as in the near wall region. In the hub region, there are typical low energy areas which are mainly caused by the wakes of previous stators (in the case of rotor 1 the IGV) and are migrating through the rotor row. They are smeared but not completely mixed out over the passage. This is visible when comparing directly the pressure contours behind rotor 3. A region of high energy fluid behind the shrouded rotor 3 can be seen, beginning on the hub and growing up to almost 60% of blade height. In the case of the cantilevered build this region is splited by the low energy fluid of the hub clearance vortex of previous stator. This area of high energy fluid begins on the hub because of the flow acceleration due to hub rotation (the cobra probe is located in both cases above the rotating hub, compare figure 3). The circumferential variation of the total pressure behind the rotors can also be caused by the upstream potential effect of the downstream stator row (this applies especially to the main flow). It is not possible to quantify both effects without an investigation of clocking effects, as mentioned before.

In the rotor tip clearance region, areas of low total pressure occur which are very similar for both builds. That means that this region does not appear to be affected by the different stator configurations.

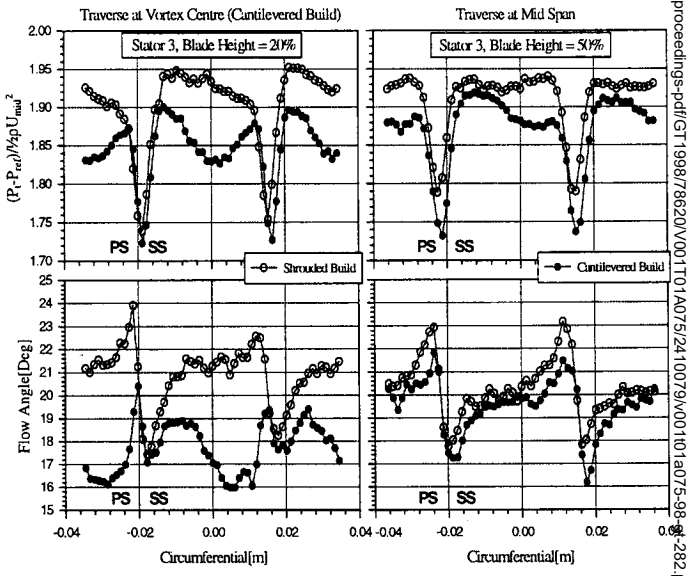

Figure 8: Measured Flow angle and total pressure at mid span traverse and at the low pressure center (cantilevered build) for stator 3 at peak efficiency operating point

Figure 8 shows the described effects more in detail by comparison of circumferential traverses at the center of the low angle/low pressure region (20% blade height) and at mid span behind the third stator. The differences in the hub region caused by the hub clearance vortex are clearly recognizable. At mid span the lower pressure level for the cantilevered build can be seen but also the different shape of both, pressure and angle curves. Thus the influence of the hub clearance flow is even present at mid span and interacts with the main flow.

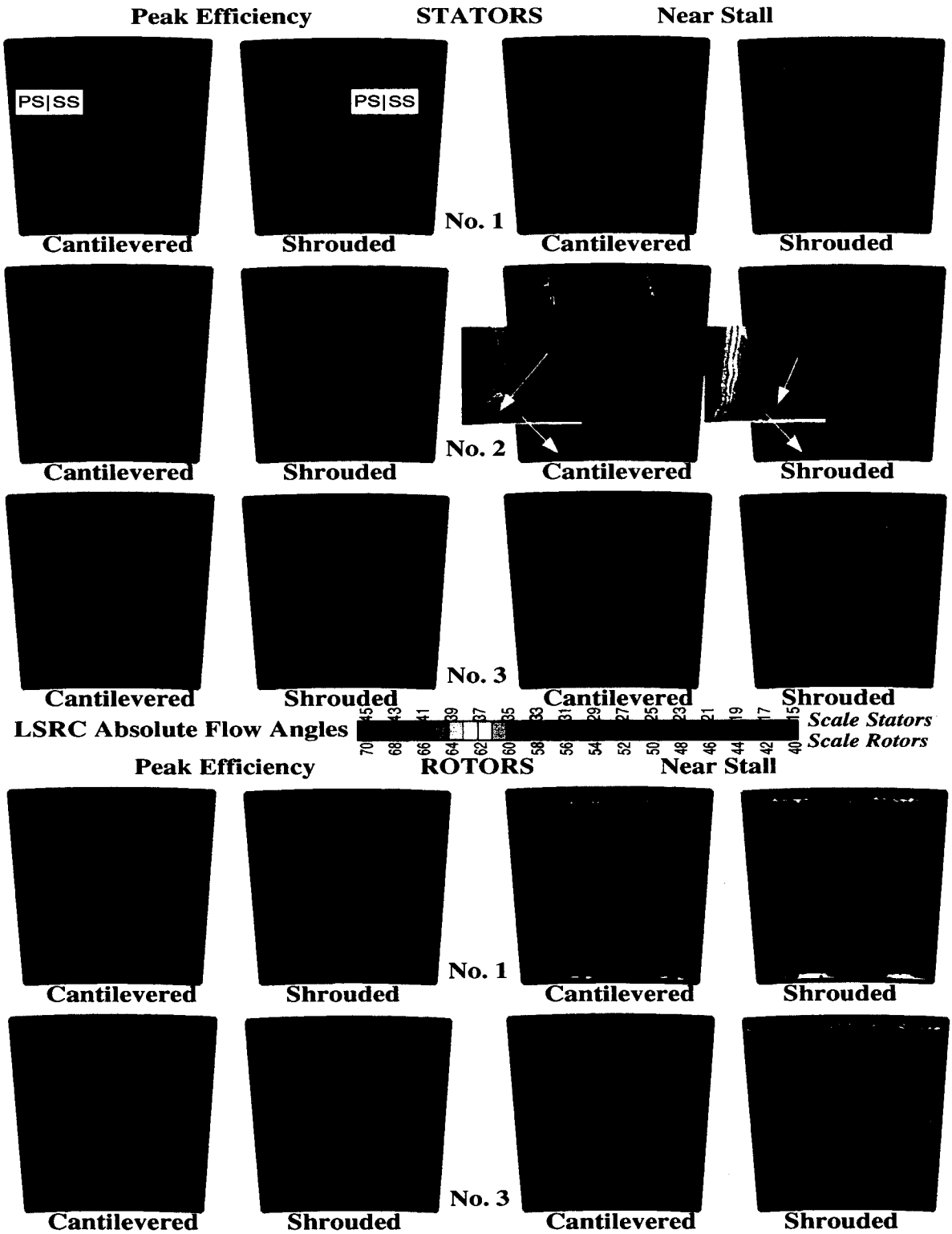

Figure 6: Distribution of absolute flow angles for all measured traverse planes, comparison between cantilevered and shrouded stators for both measured operating points

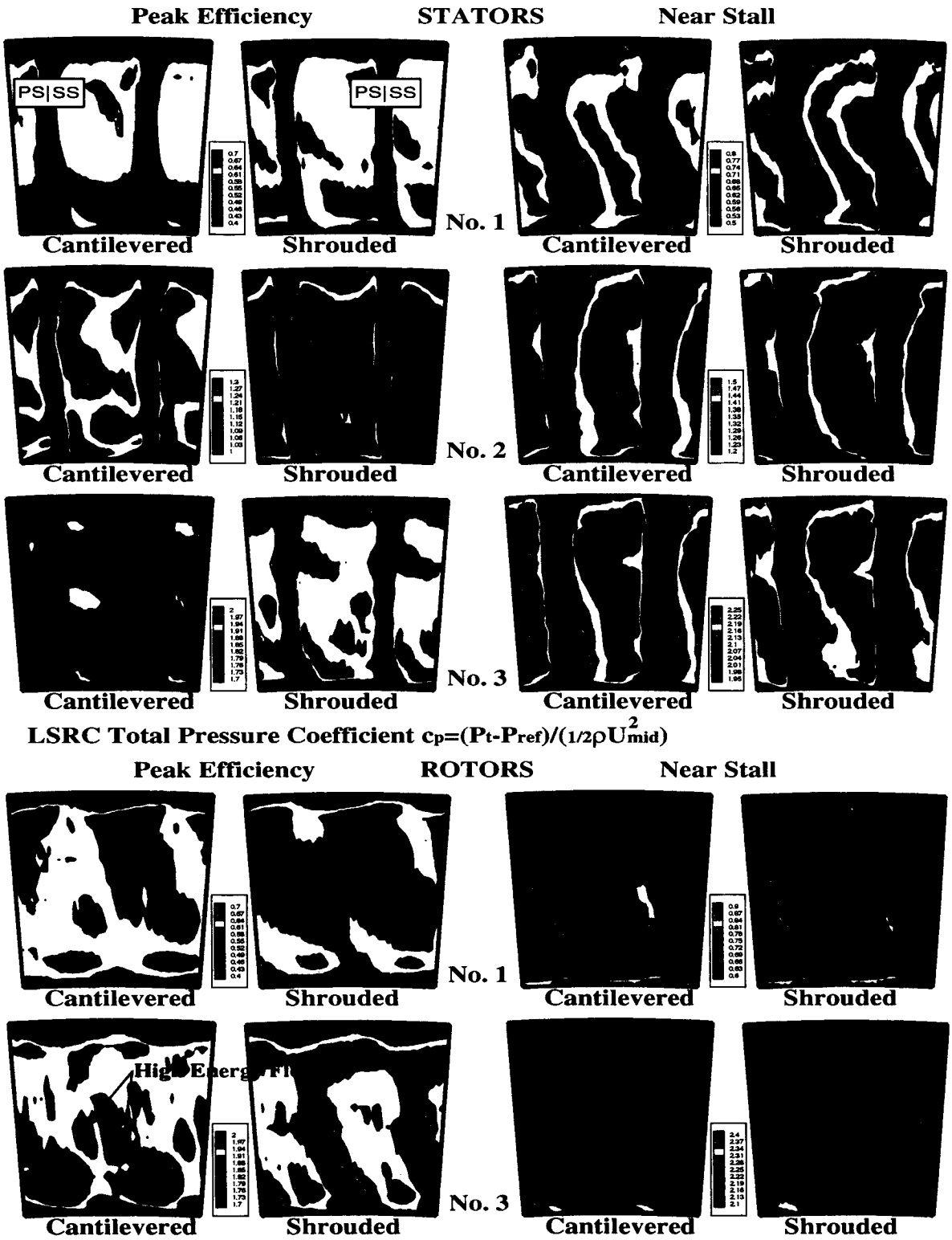

Figure 7: Distribution of total pressure coefficient for allmeasured traverse planes, comparison between cantilevered and shrouded stators for both measured operating points

To summarize the traverse measurements at peak efficiency point it can be stated that the flow field pattern is mainly governed by the hub clearance, but is also still affected by a vortex propagating from the IGV through the machine. In the case of cantilevered stators the IGV-vortex interacts with the distinct stator hub clearance vortices and intensifies towards the rear stages, whereas in the shrouded case this vortex structure is smeared out.

Near Stall Operation

The angles for the near stall case are also shown in Figure 6 for comparison reasons to the same scale. The angle range is much higher than for the peak efficiency point. Considering the traverses behind the stators it can be observed that the effect caused by the hub clearance vortices (overturning from 10 to almost 40% blade height) in the cantilevered case does not affect the flow field any more.

As already mentioned in the discussion of the overall characteristics, compressor instability is believed to be mainly triggered by stage 2. Compared to stator 1 and 3 angle contours, large separation regions near the casing can be seen behind stator 2 for both builds. This can be seen on the triangular shape of the contour lines near the casing (see enlarged drawings, figure 6). High angles (>35°) occur on the pressure side and very low angles on the suction side corner (<15°). For the build with shrouded stators, separation also occurs on the hub (same structure as on the tip) whereas there is no indication of separation on the hub in the case of cantilevered stators due to the removed separation caused by the hub clearance vortex mentioned above. Here the stronger hub clearance vortex appears to remove the separation because its rotation direction is opposite to the secondary flow passage vortex.

The traverses behind rotors show almost no differences for both builds expect of course the distinct thicker boundary layer on hub in the cantilevered case.

In Figure 7 the respective total pressure coefficient is plotted for the near stall operating point. The wakes behind the stators are much more distinct and of higher width because of partly separated flow on the suction side. The low energy fluid region caused by the hub clearance vortices (compare peak efficiency operating point) does not occur any more in the hub region of the cantilevered case. The reason for this might be the increased secondary flow covering the hub clearance vortex effects at near stall condition. However, the wakes near the hub are thinner in the case of cantilevered build showing that the hub vortices still influence the hub region. There is a high loss region (triangular shape of contours) on the suction side hub corner in the case of the shrouded build whereas in the cantilevered case fluid of higher energy is transported to the corner by the hub clearance vortex. This is probably the reason for the slightly lower flow coefficient (compare Figure 3) and thus slightly higher surge margin for the build with cantilevered stators. Comparing the total pressure traverse measurements behind the rotors there is almost no difference visible for both builds. Even the hub boundary layers look very similar in both cases. The wakes of the previous stator row propagating through the rotor row and the potential effect of the downstream stator row are more pronounced than at the peak efficiency operating point.

To summarize this, it can be stated that the cantilevered build is tip critical whereas the shrouded build is hub and tip critical with respect to stall phenomena. This observation applies only to the stator flow traverses; it is not possible to make a statement for rotors without traverse measurements near stall in rotating frame of reference.

BLADE PRESSURE DISTRIBUTION

The comparison of the blade static pressure distributions for the near wall region is shown in Figure 9. To isolate the wall effect and for comparison with the nearly undisturbed flow field also the pressure distribution at blade mid height (x/h=50%) for both builds has been plotted.

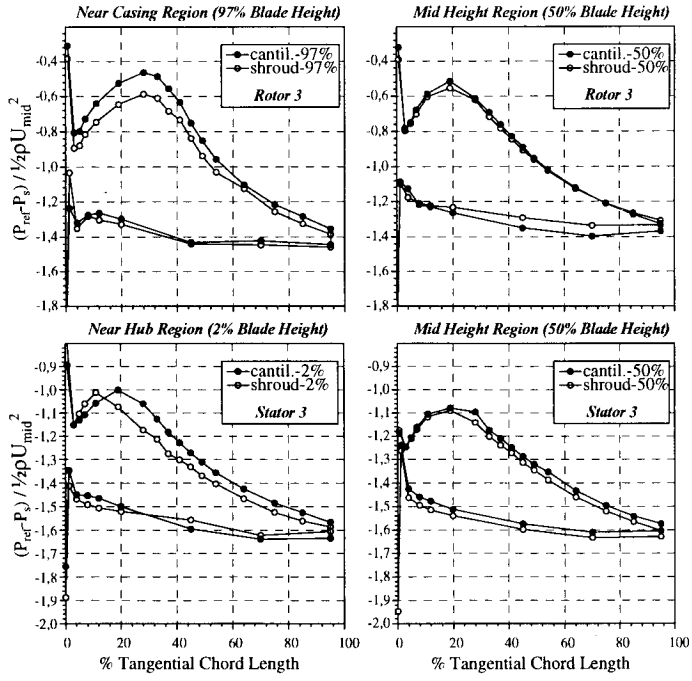

Figure 9: Blade pressure comparison for rotor 3 and stator 3 in wall and mid height region for peak efficiency operating point

In the upper half the pressure distribution for the third rotor is shown. In general both distributions in the casing region (blade height=97%) show higher blade loading and the peak of

maximum suction is shifted approximately 10% chord downstream relative to mid span. This is caused by an increase of incidence of about 8° in that region and some local mass flow increase compared to design value in both cases (compare next section, figure 11). The loading on the tip of the rotor in the case of the cantilevered build is much higher than for the shrouded build, however, the suction peak is located at the same position indicating similar incidence. This seems to be due to higher velocity on casing for the cantilevered build because a velocity deficit occurs near the hub and thus the velocity on casing increases. This is shown in figure 10 where velocity components on rotor 3 leading edge are plotted which result from the through-flow reconstruction,. Both velocity components are smaller in the near hub region (10 to 30%) and higher in the casing region (70 to 100%) for the cantilevered compared to the shrouded build.

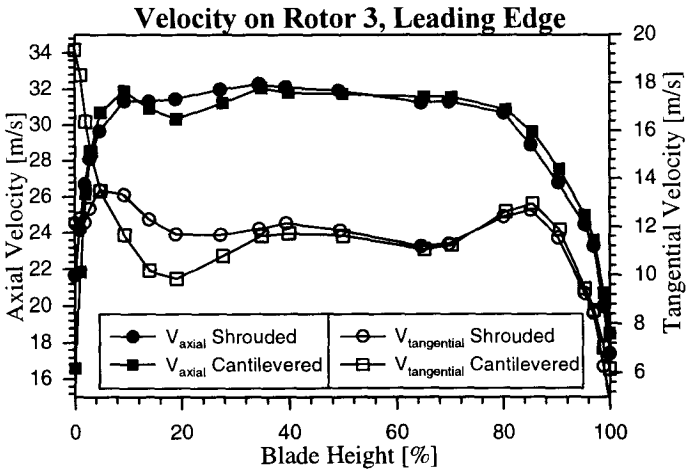

Figure 10: Velocity components on rotor 3 leading edge for both builds

The lower half of Figure 9 shows the respective pressure distributions for the hub and mid span region of the third stator. The suction pressure on hub region (blade height=2%) is in both cases - similar to the rotor tip region - higher than at mid span due to increased incidence near the hub in both cases. Although incidence appears to be reduced in the cantilevered case the loading on the hub is again somewhat higher. Load was moved rearward due to the influence of the hub clearance vortex. However, the position of the suction peak remains constant for the cantilevered build whereas it is shifted further upstream for the shrouded case relative to mid span. This is because the incidence is even higher for the cantilevered build. This can be seen when comparing the pressure distribution on the pressure side of the blade (see also figure 12).

In the mid span region of stator 3 a development of a laminar separation bubble can be observed for the cantilevered case in the region at approximately 30% of chord length which is in accordance with the design process. This is visible as the slight kink in the suction pressure distribution behind the suction peak. The static pressure here remains locally constant. There is no separation bubble visible for the shrouded build, however, if a separation bubble also exists in this case, it could be missed by the pressure taps.

THROUGH-FLOW RECONSTRUCTION

In this section some results of the through flow reconstruction analysis are presented. In Figure 11 the gas angle summary (i.e. flow angles at inlet and outlet) and losses of the third rotor at the peak efficiency operating points are drawn. Figure 12 shows these results for stator 3. For comparison also blade metal angles as well as design flow angles are given in both figures.

The viscous effects are clearly visible for both builds causing a large increase in flow angle and thus in incidence on the hub and especially on the tip for rotor 3, figure 11. The effects of the hub clearance vortex can be seen on both the leading and trailing edge of the rotor at peak efficiency point. The design flow angle on the leading edge is well reached for the rotor 3 in the case of the shrouded build almost from 10 to 80% of blade height. In the case of the cantilevered build there is a distinct increase in the hub region in the range from 10 to 30% of blade height. The inlet angle is up to approximately 3deg higher causing an increase in incidence. Consequently the deviation is growing also in this case by approximately 5deg compared to the design angle and by about 4deg compared to the shrouded case. The outlet design angle is not reached in both builds in the main flow field and thus there is a slight underturning which is even larger in the hub region (10 to 30%) for the cantilevered build.

The underturning over the bulk of the span of the rotor is causing a decrease in incidence on the following stator 3 for peak efficiency point, figure 12. Comparing both builds it can be seen that the angle distribution in the case of the cantilevered build is somewhat smoother on the hub. A typical angle distribution for stators can be seen on the stator outlet for the shrouded build. In the tip region very close to the wall there is a characteristic overturning followed by a typical underturning further away from the wall between 70 and 90% of blade height. There is almost no difference for both builds in the region between 70 and 90% of blade height. The stator outlet angle on the hub (10 to 30%) is up to 5deg lower for the cantilevered build caused again by the hub clearance vortex and therefore the blade turning here is higher compared to the shrouded build. In the near hub region the angle on hub is for the cantilevered build of course much higher (theoretically 90deg) caused by hub rotation.

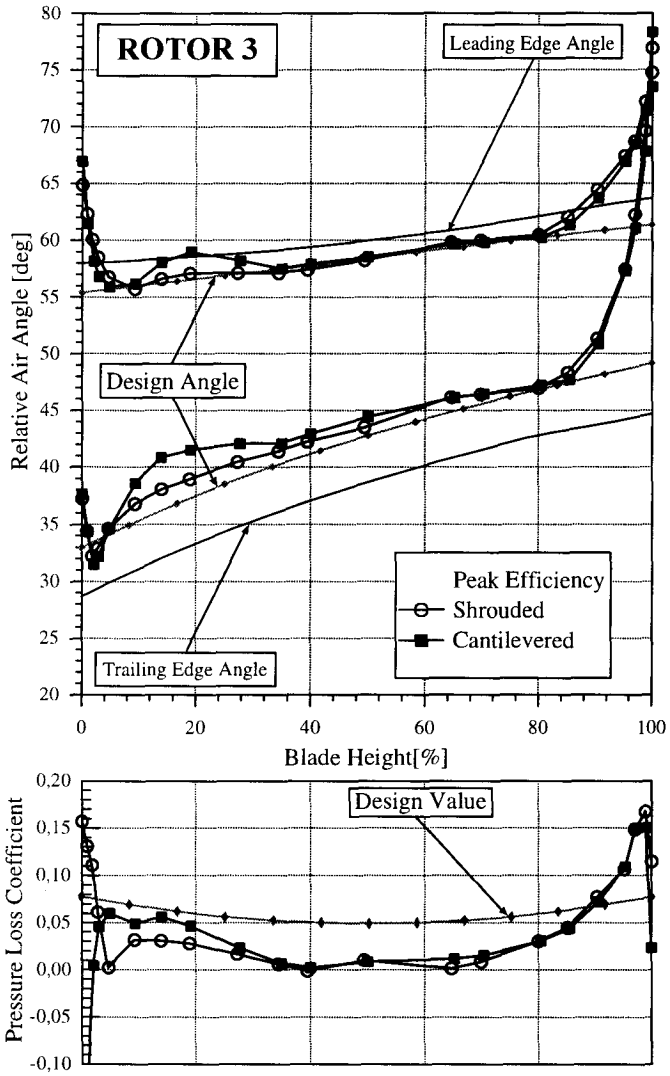

Figure 11: Through flow analysis results for rotor 3

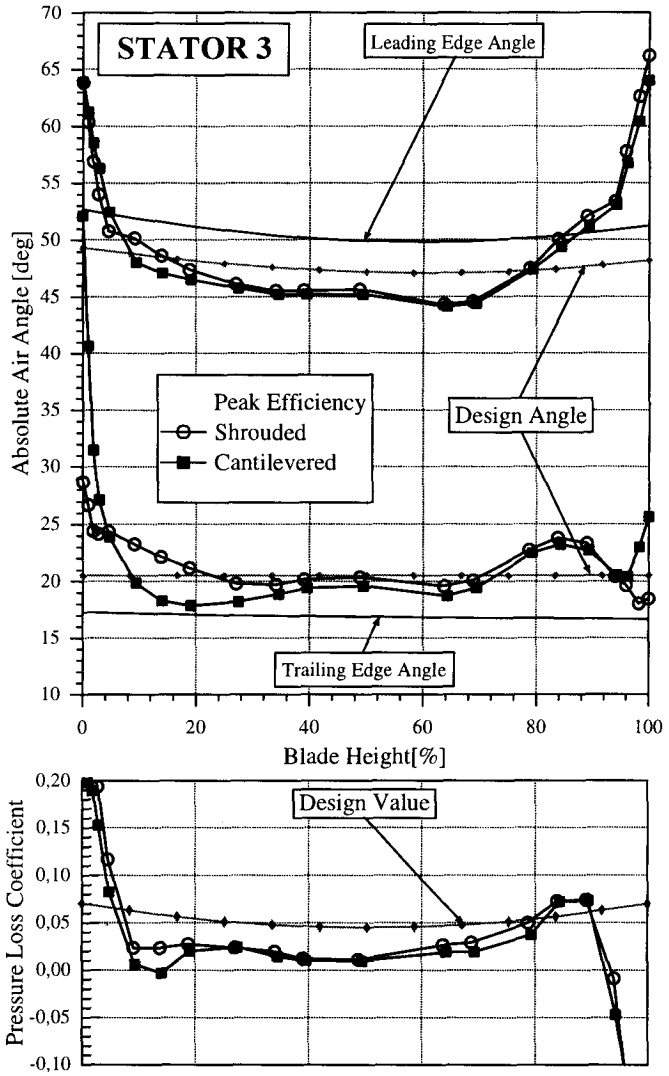

Figure 12: Through flow analysis results for stator 3

Considering the pressure losses it is visible that in general the through-flow calculation gives lower than the design assumption. The values are rather small in the mid span region. Comparing the different builds it becomes obvious that the differences occur mainly in the hub region. For the rotor the losses are higher for the cantilevered build due to the stator hub clearance vortices which change the incidence in the hub region and propagate through the rotor. In the case of the stator the losses are lower in this region for the cantilevered stator case. This is because of the continuous acceleration of the near wall flow by the rotating hub whereas the flow in the shrouded case will be decelerated throughout the shroud. Thus, it can be concluded that the cantilevered stators are beneficial to stator performance but detrimental to rotor performance.

Taking this into account in the rotor design procedure would result in better performance of the whole stage or the whole compressor. This could be achieved by redesigning the rotor profiles in the near hub region (10-30% blade height).

CONCLUSIONS

In this paper, detailed comparison has been made of the flow field in an axial compressor equipped with identical rotors but with either cantilevered and shrouded stators. The effects of the hub clearance vortex manifesting itself in affecting loss and flow angle distribution are described and compared to the shrouded configuration.

Overall performance analysis shows slightly higher work coefficients for shrouded stators, but slightly higher stall margin in the cantilevered case. This is caused by the hub clearance vortex which removes separation regions on the hub and thus stabilizes the flow field because its direction is opposite to the secondary flow in the passage. These effects are shown in detail by means of traverse measurements at peak efficiency and near stall operating point.

The through-flow reconstruction analysis of the measurements confirms the described effects. The stator losses for the cantilevered build are smaller in the hub region because of the stabilizing effect of the hub clearance vortex. The rotor losses are higher in the hub region for the cantilevered build because of changed rotor inlet flow conditions, i.e. increased incidence due to the hub clearance vortex. The rotor hub geometry could be improved during the design procedure by taking into account the effects of the hub clearance vortex on the radial distribution of flow angle and total pressure into the downstream rotor (reblade of profiles in that region). The performance of the whole machine could be improved for cantilevered stators.

The presented measurements are of high quality and are perfectly appropriate for validation of 3D Navier Stokes codes, whose acceptance is growing to use as compressor design methods.

ACKNOWLEDGEMENTS

The project was funded by the European Community, Rolls Royce, Snecma, BMW Rolls Royce, Turbomeca and MTU as a BRITE/EURAM (Project AC3A) Contract AER2-CT92-0039, which was monitored by Dr. R. Dunker and Dr. W. Borthwick. The authors would like to thank BMW Rolls Royce GmbH for the permission to publish this work. The authors would also like to thank Dr. T. Camp, Rolls-Royce plc who advised the presented through-flow calculations.

REFERENCES

Adams, N. G.: „Flow Visualization Study of Tip Leakage Flows Across Cantilevered Stator Blades", AIAA Journal of Propulsion and Power, Vol. 4, No. 2, Mar.-Apr. 1988, p 144-151, 1988

Brankiewicz W. S., Hathaway M. D.: „Impact of Variable Geometry Stator Hub Leakage in a Low Speed Axial Compressor", to be published at ASME Turbo Expo Stockholm 1998

Camp, T. R.: Cranfield Tare-Torque Calibrations for the Processing of BRR Data, Internal Memorandum, Rolls Royce Sin A-43, 1996

Dring, R. P., Joslyn, H. D.: „The Effects of Compressor Endwall Flow on Airfoil Incidence and Deviation", AGARD CP 469, paper No. 2, 1989

Goto, A.: „Three Dimensional Flow and Mixing in Axial Flow Compressor with Different Rotor Tip Clearances", ASME conference paper 91-GT-89, Orlando, 1991

Heidegger N. J., Hall E. J., Delaney R. A.: „Parametrized Study of High-Speed Compressor Seal Cavity Flow", AIAA Paper 96-2807, July 1-3, 1996

Howard, M. A., Ivey, P. C., Barton, J. P., Young K. F.: „Endwall Effects at Two Tip Clearances in a Multi-stage Axial Flow Compressor with Controlled Diffusion Blading", ASME J. of Turbomachinery, V116, No.4, p635-647, 1994

Ivey, P. C., Swoboda, M.: „Leakage Effects in the Rotor Tip-Clearance Region of a Multistage Axial Compressor, Part 1: Innovative Experiments", to be published at ASME Turbo Expo Stockholm 1997

Jung, M., Eickelmann, J.: „Stator Exit Flow Fields in the Multistage Environment of an Axial Compressor", ASME Conference paper 95-GT-165, 1995

Jefferson J. L., Turner R.C.: „Some Shrouding And Tip Clearance Effects in Axial Flow Compressors", Int. Ship Building Progress, Vol. 5, No. 42, Feb. 1958

LeJambre, C. R., Zacharius, R. M., Biederman, B. P., Gleixner, A. J., Yetka, J.: „Development and Application of a Multistage Navier Stokes Solver (part 2: Application to a High Pressure Compressor Design", ASME Conference paper 95-GT-343, Houston, 1995

Nikolos, I. K., Douvikas, D. I., Papailiou, K. D.: „Theoretical Modeling of Relative Wall Motion Effects in Tip Leakege Flow", ASME Paper, 95-GT-88, 1995

Robinson, C. J.: „Endwall Flows and Blading Design for Axial Flow Compressors", PhD Th., Cranfield Univ., UK, 1991

Robinson, C. J.: „Measurement of the Vortex Flows in a Low-Speed Axial Flow Compressor", AIAA-85-1360, 1985

Swoboda M., Wenger U., Gümmer V.: „BRITE EURAM (Project AC3A) Blading Design Report for the 4-Stage CU (Cranfield University) Low Speed Research Compressor (LSRC)", Brite Euram Report 11-BRR-02, 1996

Thompson, D. W., King, P. I., Rabe, D. C.: „Experimental Investigation of Stepped Gap Effects on the Performance of a Transonic Axial-Flow Compressor Rotor", ASME Conference paper 97-GT-7, Orlando, 1997

Wellborn, S. R., Okiishi, T. H.: „Effects of Shrouded Stator Cavity Flows on Multistage Axial Compressor Aerodynamic Performance", NASA CR 198536, Oct. 1996